

ELEMENT TRANSPORT AND PARTITIONING ALONG TIDAL CHANNELS IN SOUTHWEST BANGLADESH

Supporting Information

Authors: Matthew Dietrich^{a1} and John C. Ayers^a

^aDepartment of Earth and Environmental Sciences, Vanderbilt University, 5726 Stevenson Center, 7th floor, Nashville, TN 37240, United States

¹Corresponding Author: mjdietri@iu.edu

Text B1—Sample incubation time correlation results and suspended vs dissolved load concentrations

There are mostly poor linear trends with significant scatter between element concentrations in the suspended and the dissolved load (Fig. B10). When comparing the lab filtered samples (0.2 μm) in this study with duplicates filtered in the field (0.45 μm) from a companion study (Dietrich & Ayers, 2021), Co and Ni in the lab filtered samples are significantly elevated in concentration, along with Cr, Zn and Cu (Fig. B11). Most other elements are similar in concentration. Additionally, Co and Ni have slight negative trends between the dissolved and solid load concentrations (Fig. B10). No trends are seen between Co and Ni K_d values and time from sampling to filtration (Fig. B12). There is little correlation between days from sampling to filtration and concentrations of almost all elements in the dissolved and solid load except for Se, Mn, Cr, and V in the dissolved load (Figs. B4 & B5). An element of interest in this study, Se, does show a moderate negative correlation between days from sampling to filtration and dissolved concentration (Fig. B13).

Text B2—Discussion of possible effects of sample incubation time on the geochemistry of samples and interpretation of results

Most trace elements that may undergo desorption or dissolution processes showed significant scatter between the dissolved and suspended loads, suggesting disequilibrium partitioning (Fig. B10). Thus, even though the suspended sediments were in contact with the water for an extended period of time, slow kinetics likely prevented exchange equilibrium and any changes in water or sediment concentration were likely less than an order of magnitude. Because many of our interpretations are based on geochemical changes greater than an order of magnitude (i.e., K_d values and dissolved concentrations of Se), any sample incubation effects were likely less than the observed changes. Also, the residence time of water in the tidal channel during which reactions between sediment and water can occur was likely similar in magnitude to sample incubation time, because most water in this area is tidally reworked (Hale et al., 2019). Thus, any alterations to water and sediment chemistry from their interactions with one another likely occurred prior to our sampling and laboratory storage, especially because the salinity front in the dry season extends north past Khulna and our sampling area, where our samples first experienced freshwater-saltwater interactions and possible ionic exchange. Lastly, because of the highly saline nature of the waters, lack of significant headspace in the sealed samples during storage, sample refrigeration for the majority of sample storage time, and relatively low DOC compared to world rivers (Gaillardet et al., 2014), biological reactions were also likely limited. This was additionally shown by poor correlation between DOC and days from sampling to filtration (Fig. B4).

Specifically regarding Ni and Co Kd values, the lack of any trends with days from sampling to filtration (Fig. B12) suggests that the desorption from salt cations occurred predominantly before the samples were stored or in the early stages of storage, which would resemble real-world processes of increased residence time from additional tidal reworking or irrigation into ponds. Apparent Kd values would have the highest uncertainties for elements affected by sample incubation because concentrations in water and sediment change in opposite directions. Post-sampling effects of Se however, are possible, although there is lack of sufficient evidence to conclude that a significant amount of Se was sorbed, desorbed, or co-precipitated on suspended sediment during sample storage. The first line of insufficient evidence is the lack of exchange equilibrium between measurable dissolved and suspended Se (Fig. B10). Second, there is only a slight negative correlation ($r^2 = 0.48$; Fig. B13) between dissolved Se and the days from sampling to filtration. If there was a strong effect on the dissolved Se during sample storage, one would expect the correlation to be stronger, particularly if Se ranged 2 orders of magnitude in the dissolved load (Table 2). Third, when excluding four samples from the separate “non-effluent” 24-hour sampling period, Se is more strongly linearly correlated with salinity ($r^2 = 0.76$) relative to days from sampling to filtration ($r^2 = 0.25$), implying the trends are indeed from mixing with seawater and not induced by sample incubation. Lastly, Se concentrations in duplicate samples filtered in the field for samples MD-TC-18 and MD-TC-19 were 15 $\mu\text{g/L}$ and 30 $\mu\text{g/L}$, respectively, both less than any lab-filtered samples in this study taken during the proposed 24-hour effluent release event. Thus, even if some of the dissolved Se became immobilized in the solid phase during incubation (as suggested by the negative correlation between dissolved Se and days to filtering), the dissolved concentrations from the field filtrations (taken in the second, “non-effluent” 24-hr period) are still lower than all the Se concentrations in the main 24-hr

sampling period, supporting our Se anthropogenic effluent interpretations. However, slight sorption/desorption or coprecipitation of Se during sample storage cannot be fully discounted, particularly because of the differences in concentrations of Se in duplicate field filtered and lab filtered samples (Fig. B11) and that several other redox sensitive metals (Cr, V, and Mn) showed moderate negative correlations with days from sampling to filtration (Fig. B4).

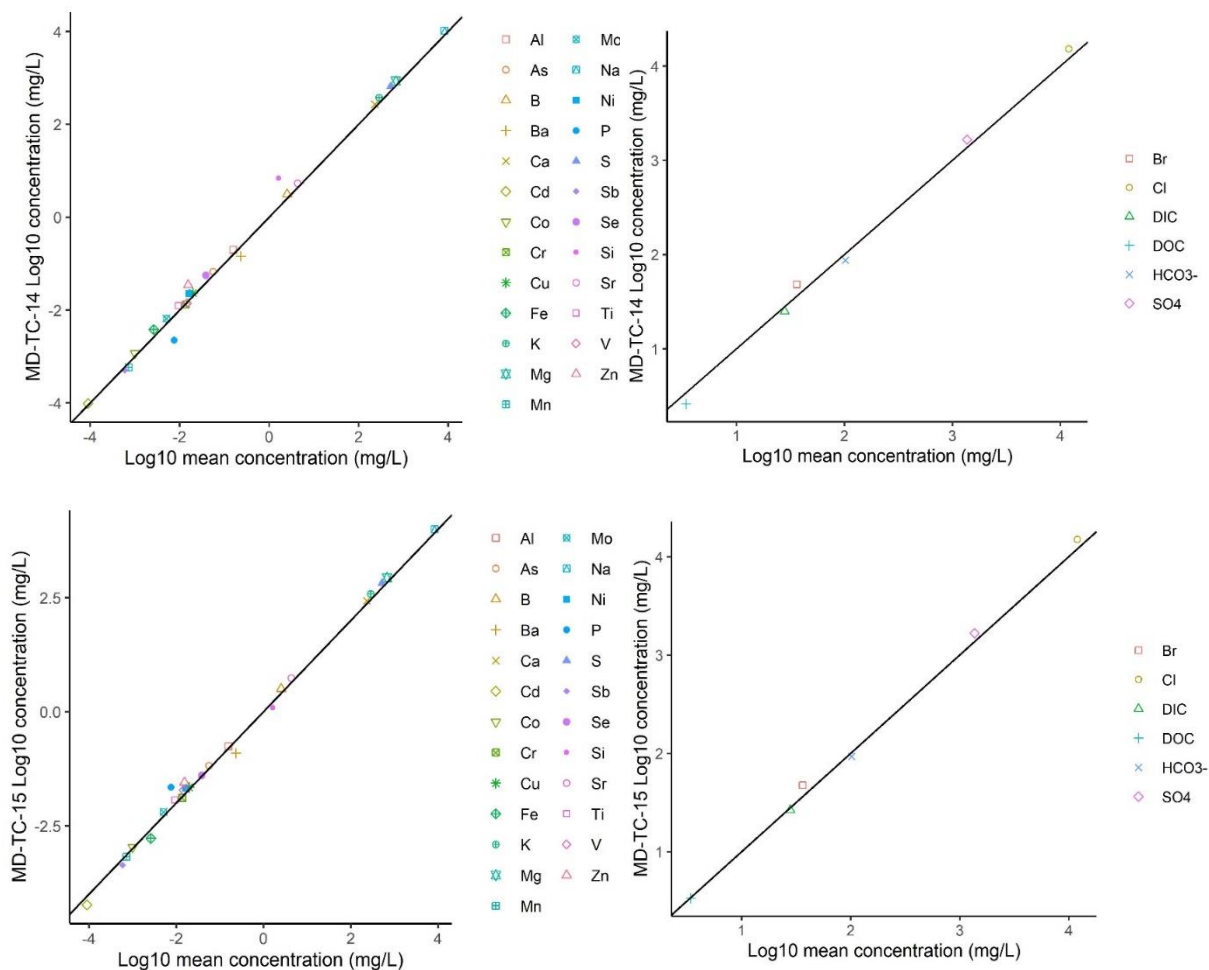


Figure B1: Log10 element concentrations in metal buckets versus log10 mean concentrations of elements in plastic buckets, with a 1:1 ratio line inserted in black.

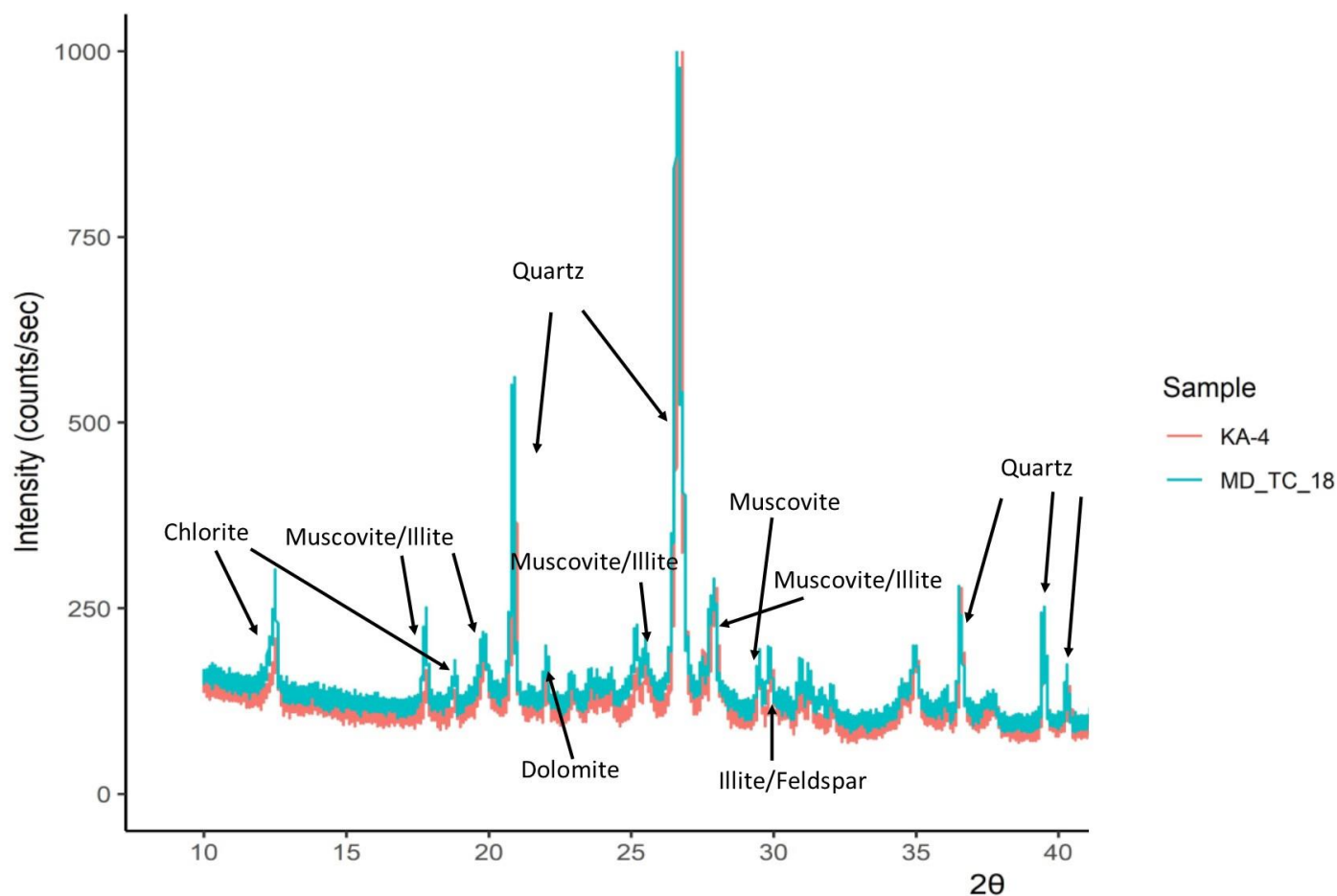


Figure B2: Powder XRD analysis of suspended sediment ($>2.5\mu\text{m}$) in the upper 1m of a tidal channel (MD-TC-18) and a shrimp pond sediment sample (Location KA-4; Dietrich and Ayers, 2021) in Southwest Bangladesh. Major mineral phases are identified with their corresponding peaks. Feldspar is a K-component of Feldspar – K ($\text{Al Si}_3 \text{O}_8$). The y-axis depicts observed intensity and is truncated for better visualization.

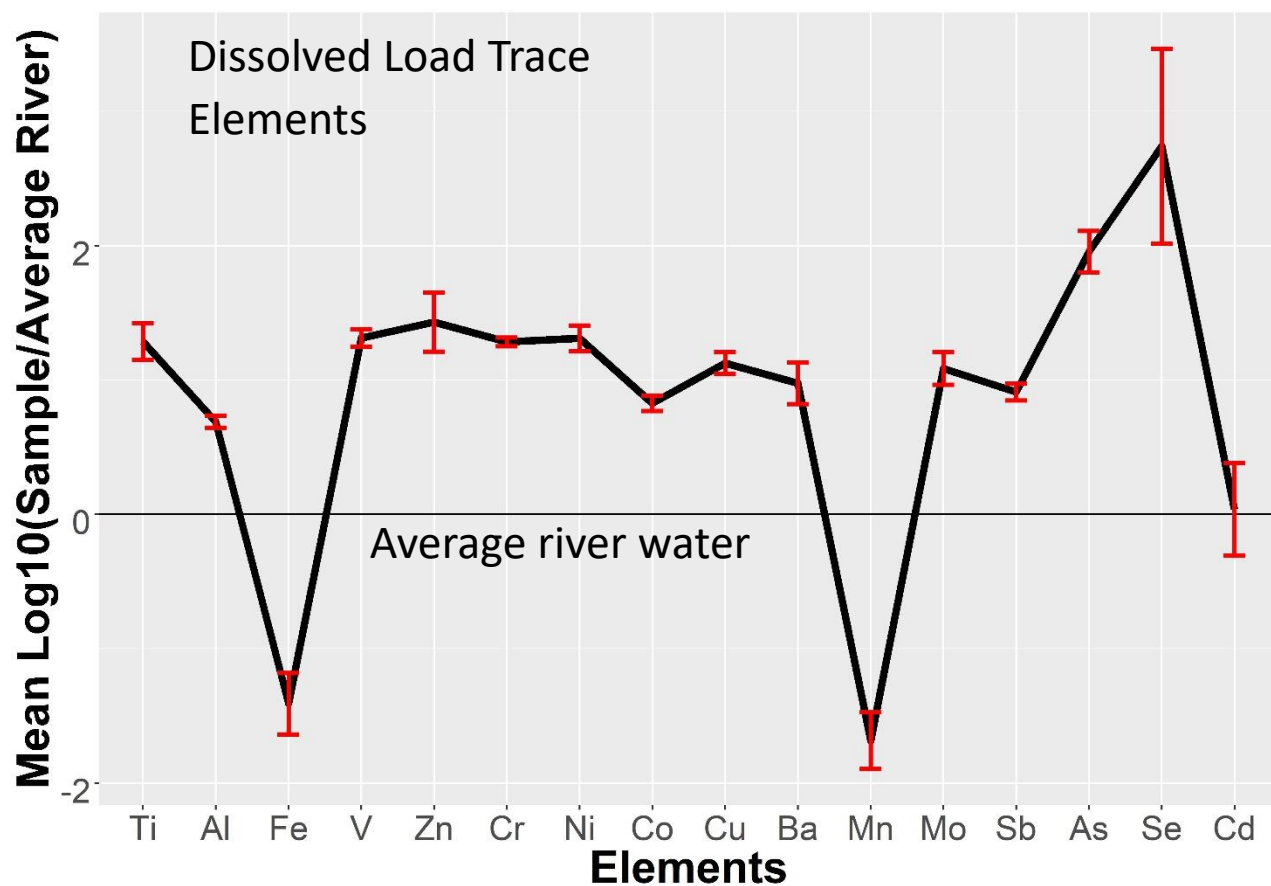


Figure B3: Dissolved element concentrations normalized to average riverine element concentrations (Gaillardet et al., 2014) with 1 σ variation error bars.

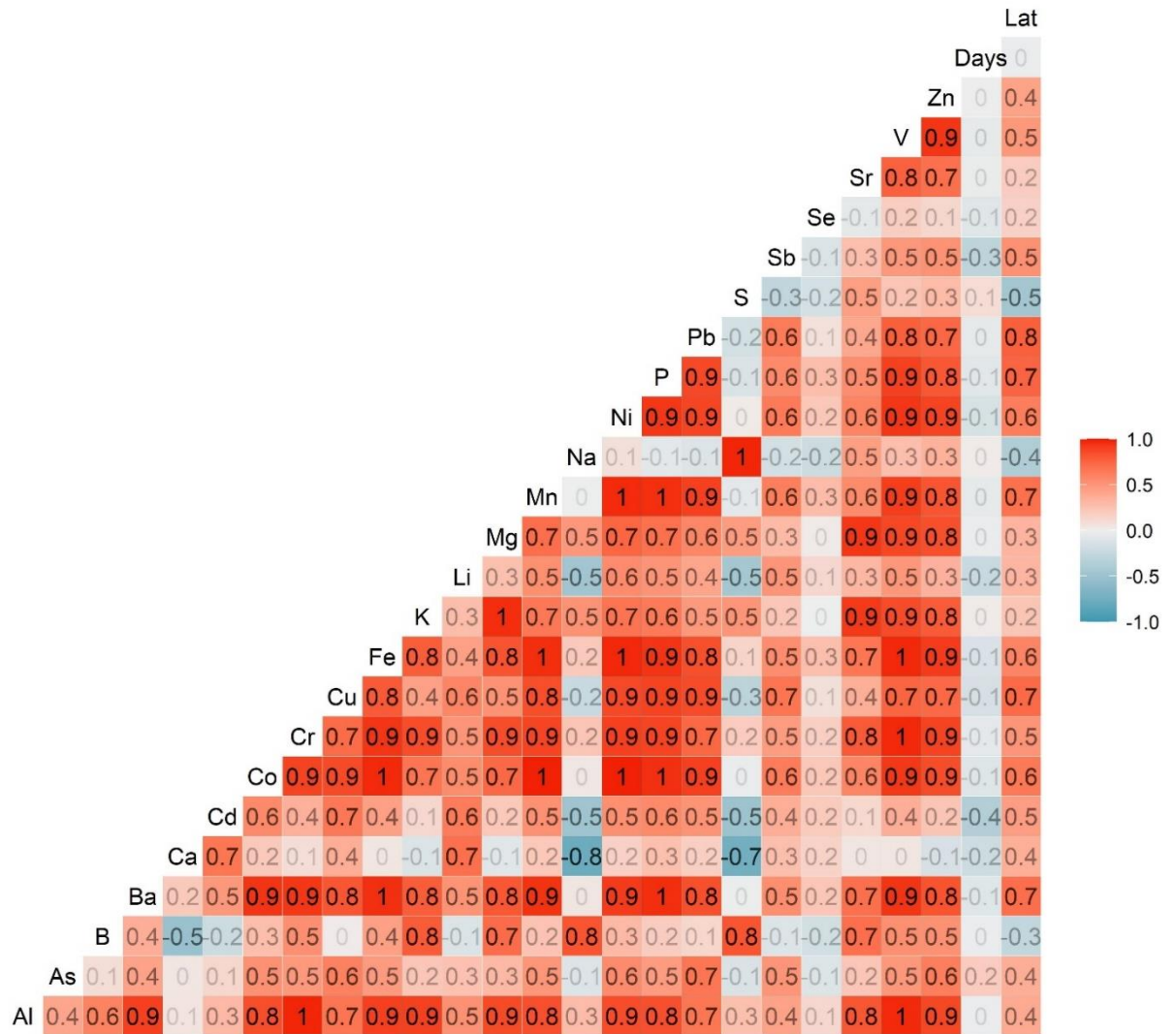


Figure B5: Suspended sediment load Spearman Rank correlation matrix (several elements are non-normally distributed) with color bar scale (detection limit values substituted in for element values <MDL). “Days” stands for days from sampling to lab filtration and “Lat” for latitude.

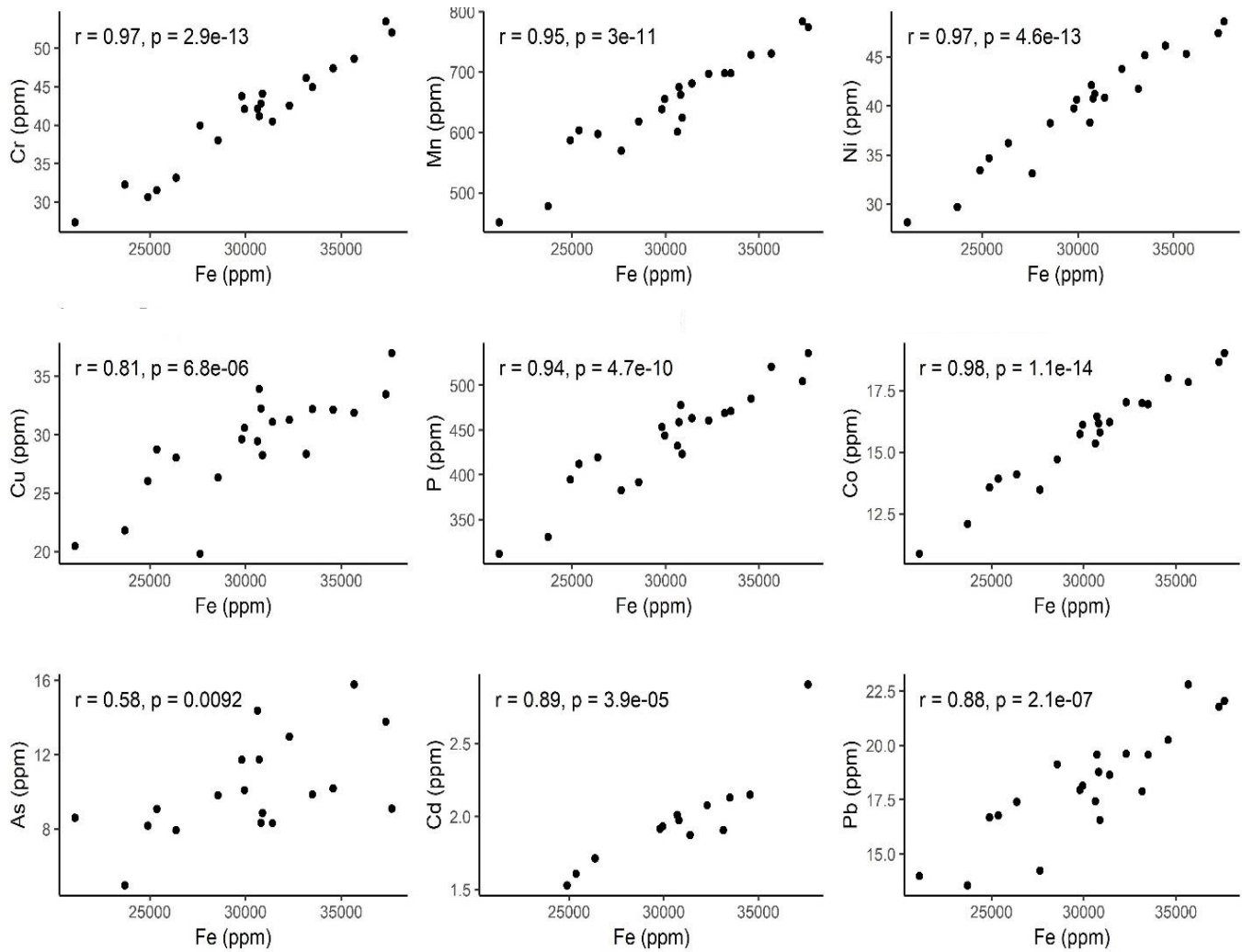


Figure B6: Several elements that showed significant positive correlations with Fe in the suspended sediment load. Concentrations <MDL are excluded. Pearson correlation coefficients and p-values are given.

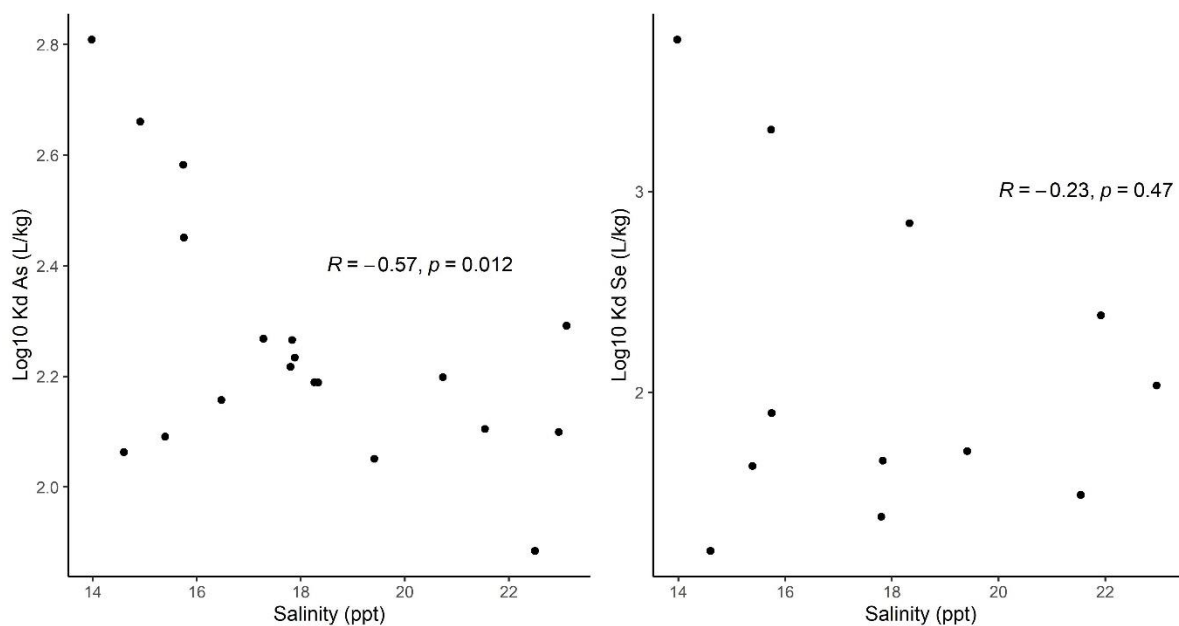


Figure B7: Salinity trends of As and Se Kd values in Log10 (L/kg) (results <MDL excluded) along the transect with increased seawater mixing. Pearson correlation coefficients and p-values are given.

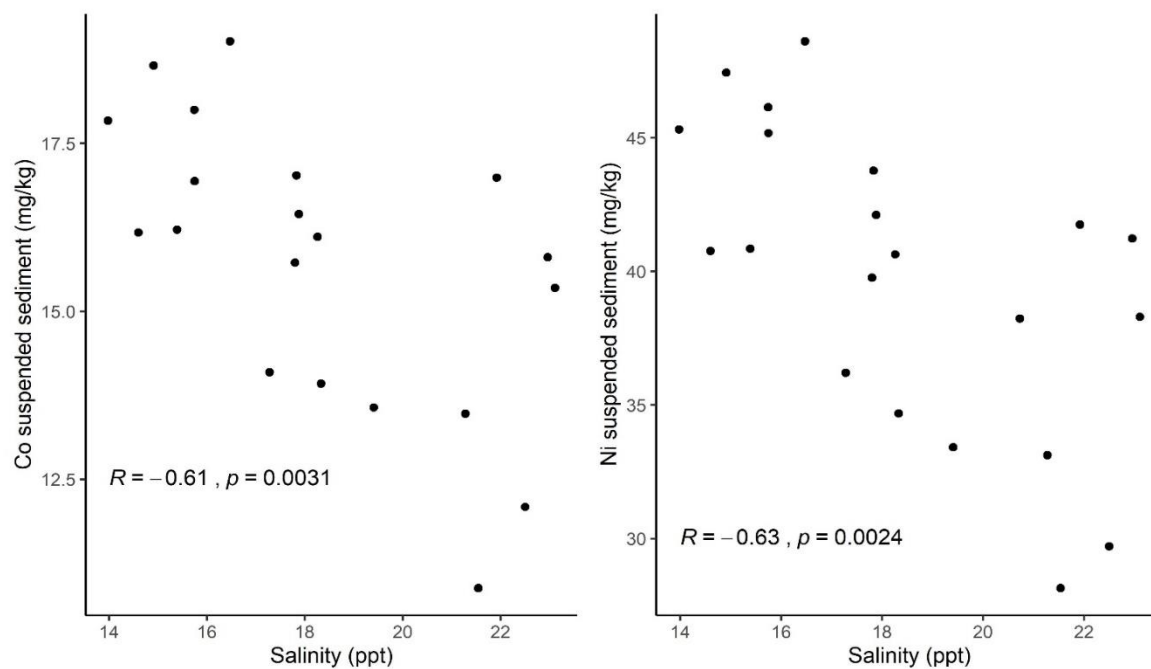


Figure B8: Cobalt and nickel suspended sediment concentration plotted against salinity, with Pearson correlation coefficients and p-values.

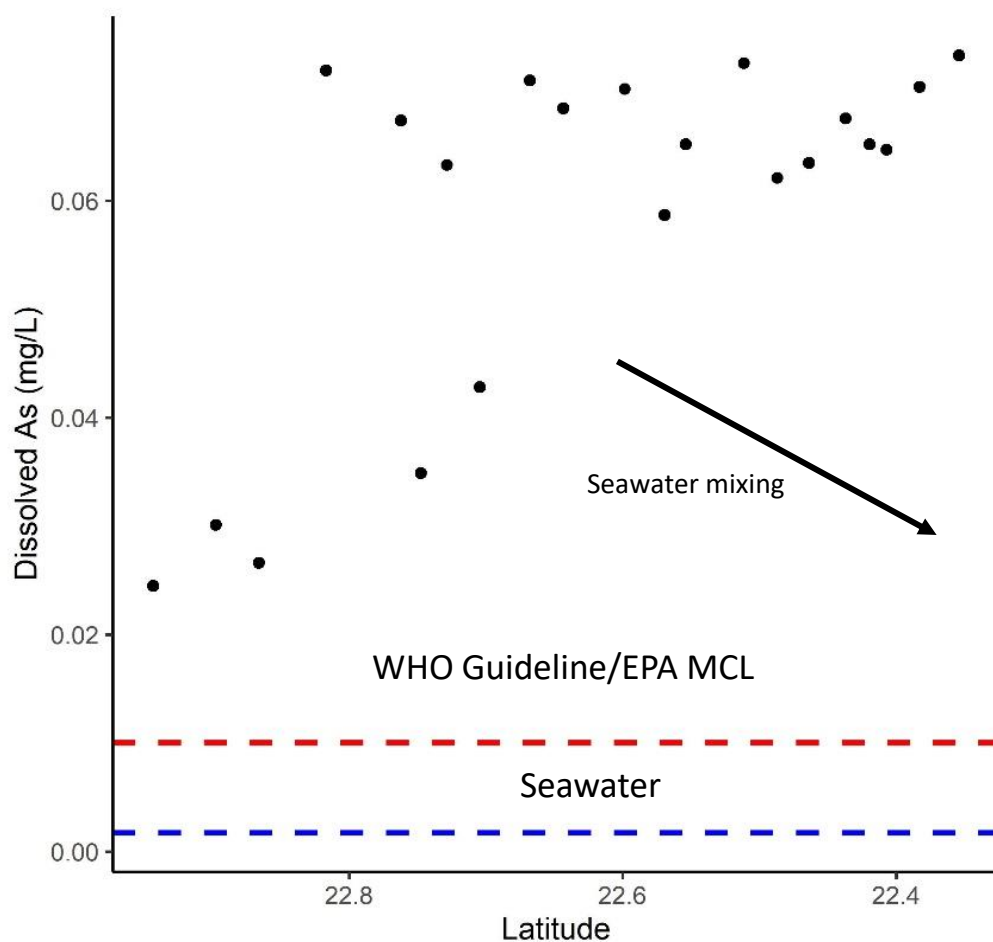


Figure B9: Dissolved As versus latitude. Correlation coefficients are omitted because of the anchoring effect of the three high latitude values in the Bhairab River. Large scatter with no definitive trend is apparent between all other samples. Average open seawater As is 0.0017 mg/L (Mason, 2013) and is marked by the blue dashed line, while the WHO guideline/EPA MCL (0.01 mg/L) is marked by the red dashed line.

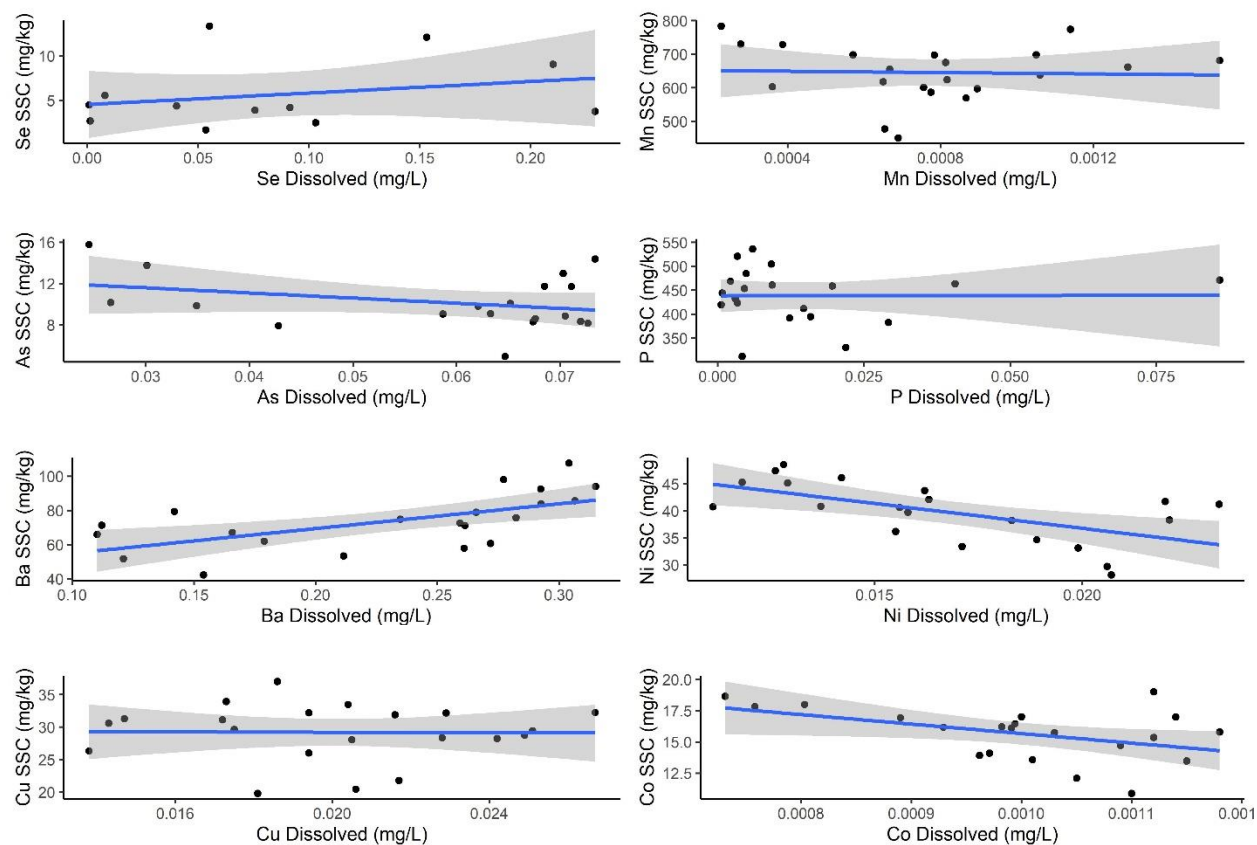


Figure B10: Element concentrations in the suspended sediment (SSC) load versus concentrations in the dissolved load. Values <MDL are omitted. The shaded gray regions represent the 95% confidence interval about the linear regression line, with linear regression statistics omitted because of the large scatter in the data (as seen with large confidence intervals).

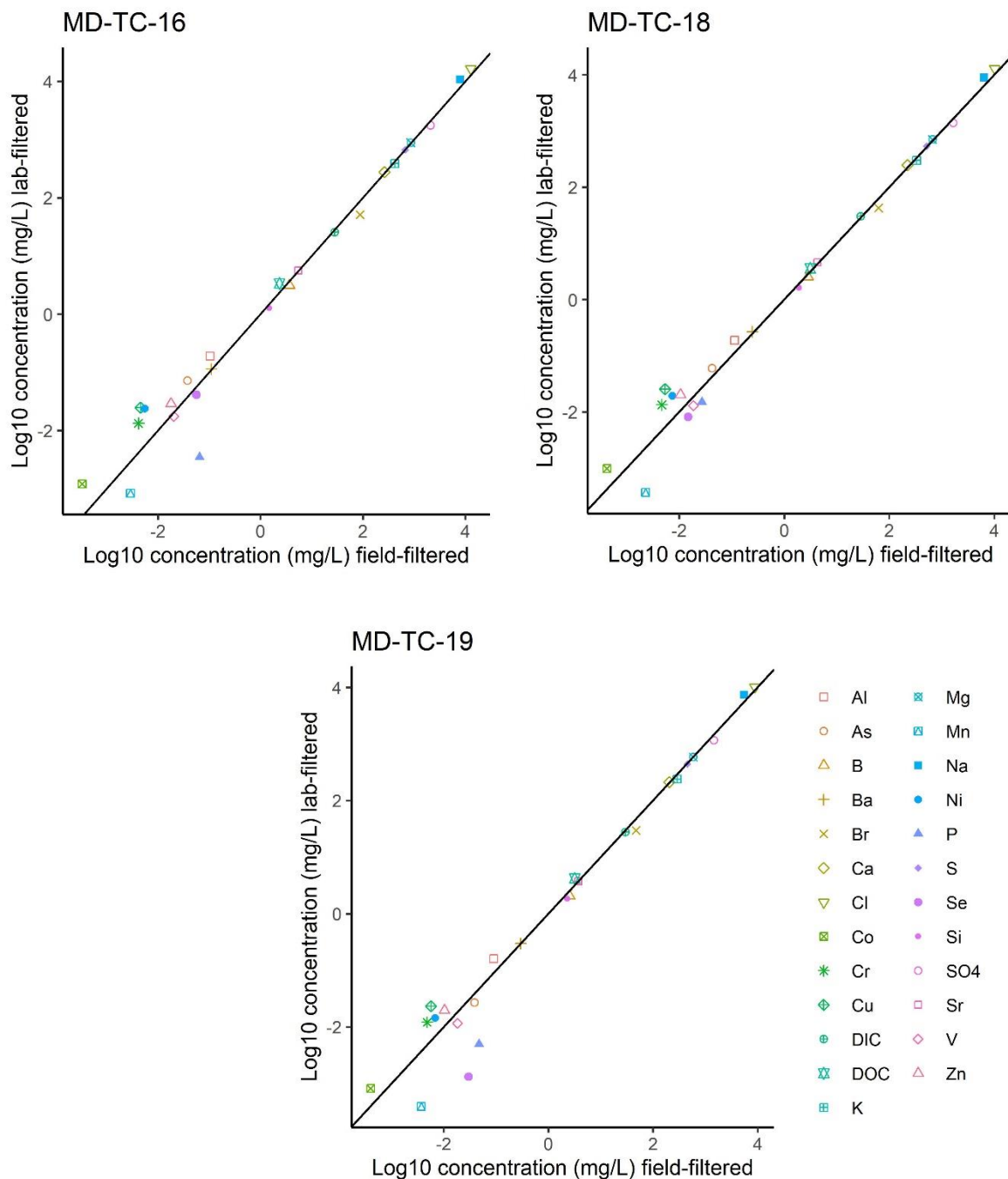


Figure B11: Comparison of field filtered dissolved load concentrations (0.45 μ m; Dietrich and Ayers, 2021) with lab filtered dissolved concentrations (0.2 μ m; This study). Each set of samples were at the same study site. Black lines are for 1:1 comparison between sample types, with a slope of 1 and y-intercept of 0. Samples falling on the black line indicate the same concentrations in both sets of samples.

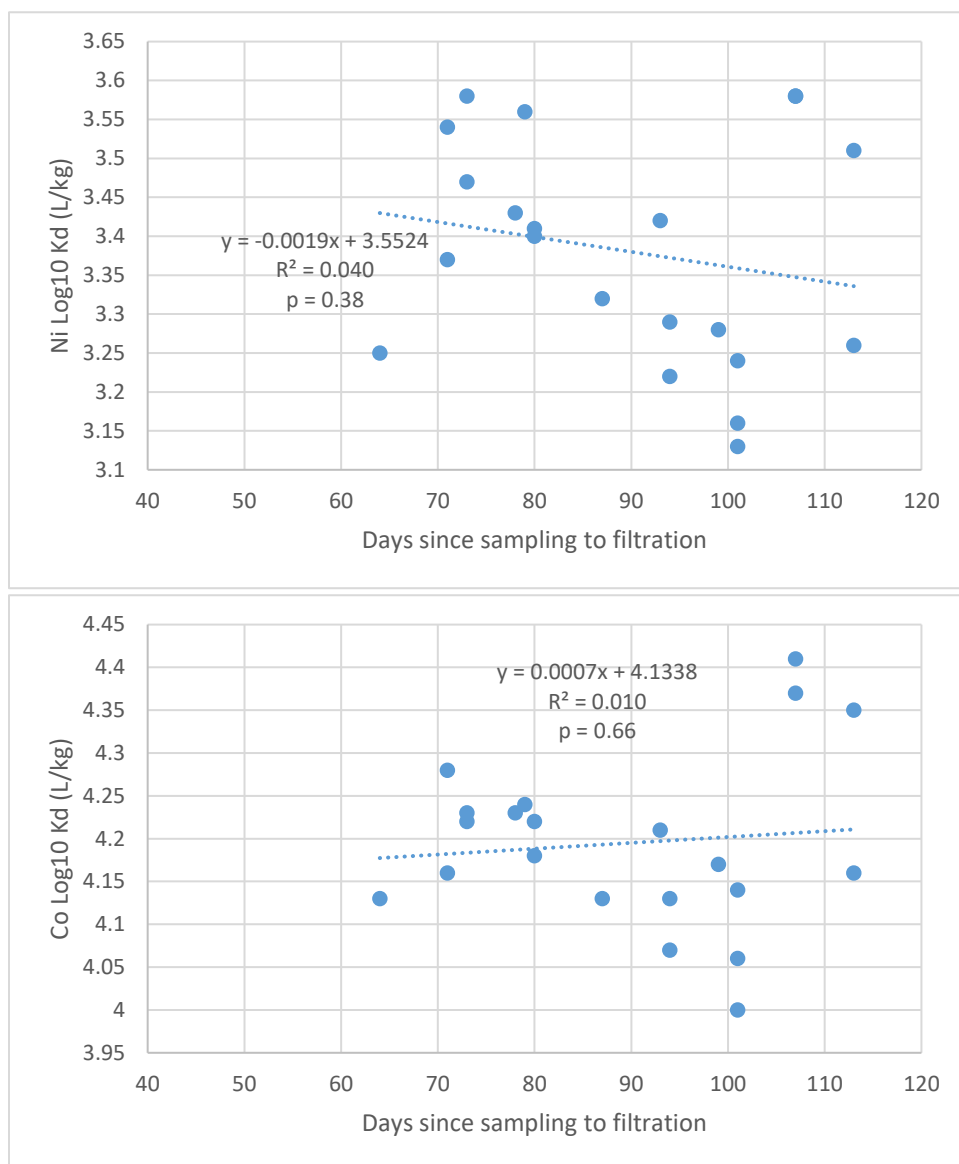


Figure B12: Days since sampling to lab filtration versus Co and Ni Kd values. Linear regression lines are provided.

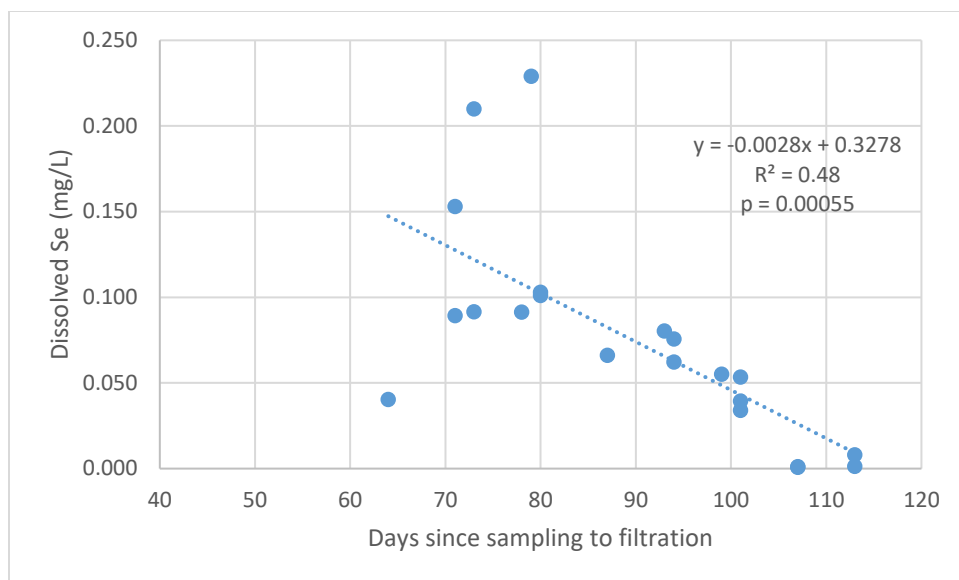


Figure B13: Days since sampling to lab filtration versus the dissolved Se concentration. The linear regression line is provided.

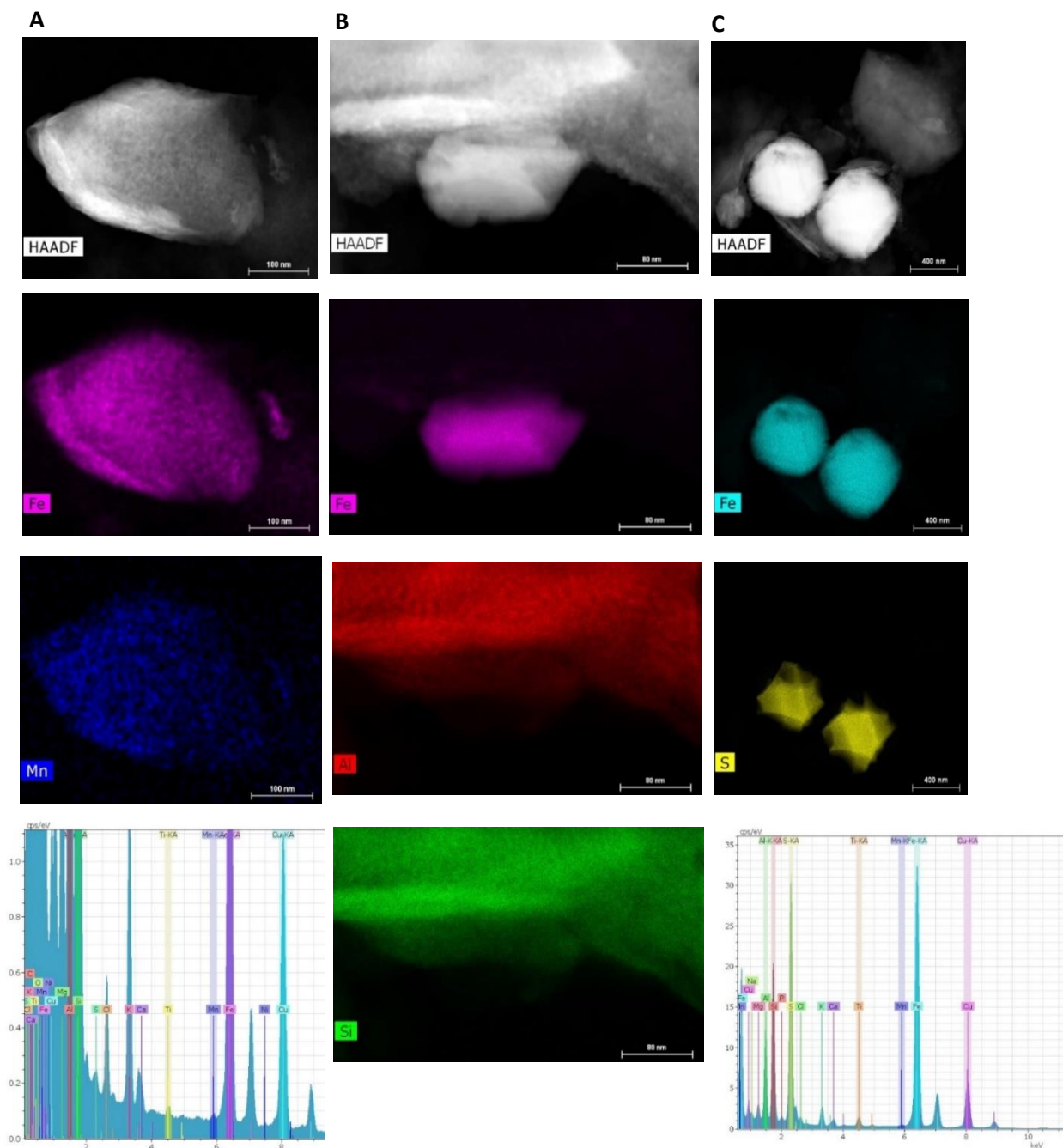
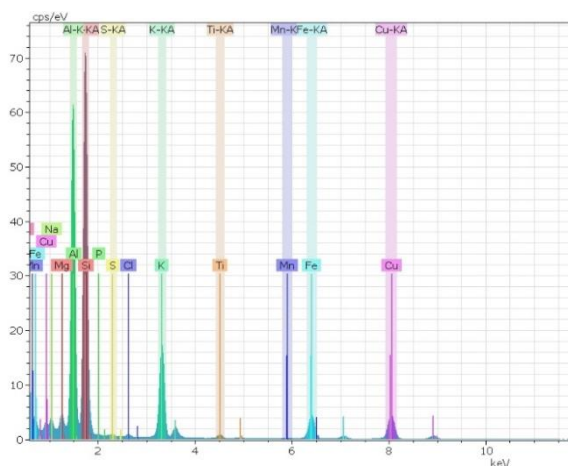
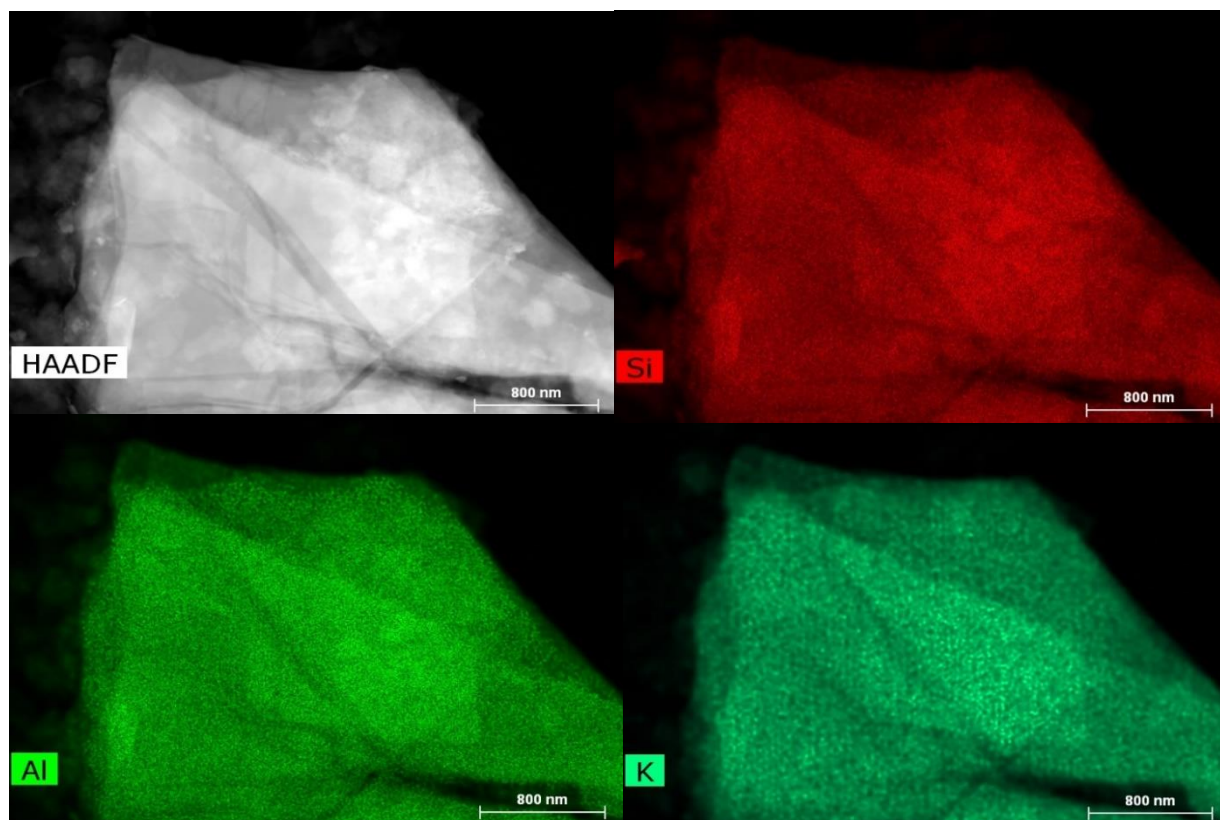


Figure B14: TEM analysis of several Fe-rich particles from samples MD-TC-7 (first two columns) and MD-TC-11 (third column), specifically showing: Column (A) – High-angle annular dark-field (HAADF) image, STEM-EDS maps, and EDS spectra with several element peaks identified for an Fe-rich particle (about 0.5 μm in diameter) associated with several transition metals such as Mn, Ti, Cu, and potentially Ni; Column (B) – HAADF image and STEM-EDS maps of Al, Si and Fe, showing the Fe-rich nanoparticle ($\sim 0.2 \mu\text{m}$ in diameter) associated with the larger aluminum silicate particle; Column (C) – HAADF image, STEM-EDS maps and EDS spectra, showing an Fe-sulfide particles $\sim 0.5 \mu\text{m}$ in diameter.



Element	series	Net	[wt.%]	[norm. wt.%]	[norm. at.%]	Error in wt.% (3 Sigma)
Silicon	K-series	298063	27.35	27.35	21.33	0.23
Aluminium	K-series	250267	22.88	22.88	18.57	2.14
Potassium	K-series	104185	9.93	9.93	5.56	0.97
Oxygen	K-series	447671	39.84	39.84	54.54	3.67
		Sum:	100	100	100	

Figure B15: TEM imaging of a K-silicate particle, potentially muscovite with other small crystals/oxides present, from sample MD-TC-11 with: a high-angle annular dark-field (HAADF) image, STEM-EDS maps, EDS spectra, and approximate wt.% and at. % concentrations of major elements present, assuming other contributions are relatively negligible.

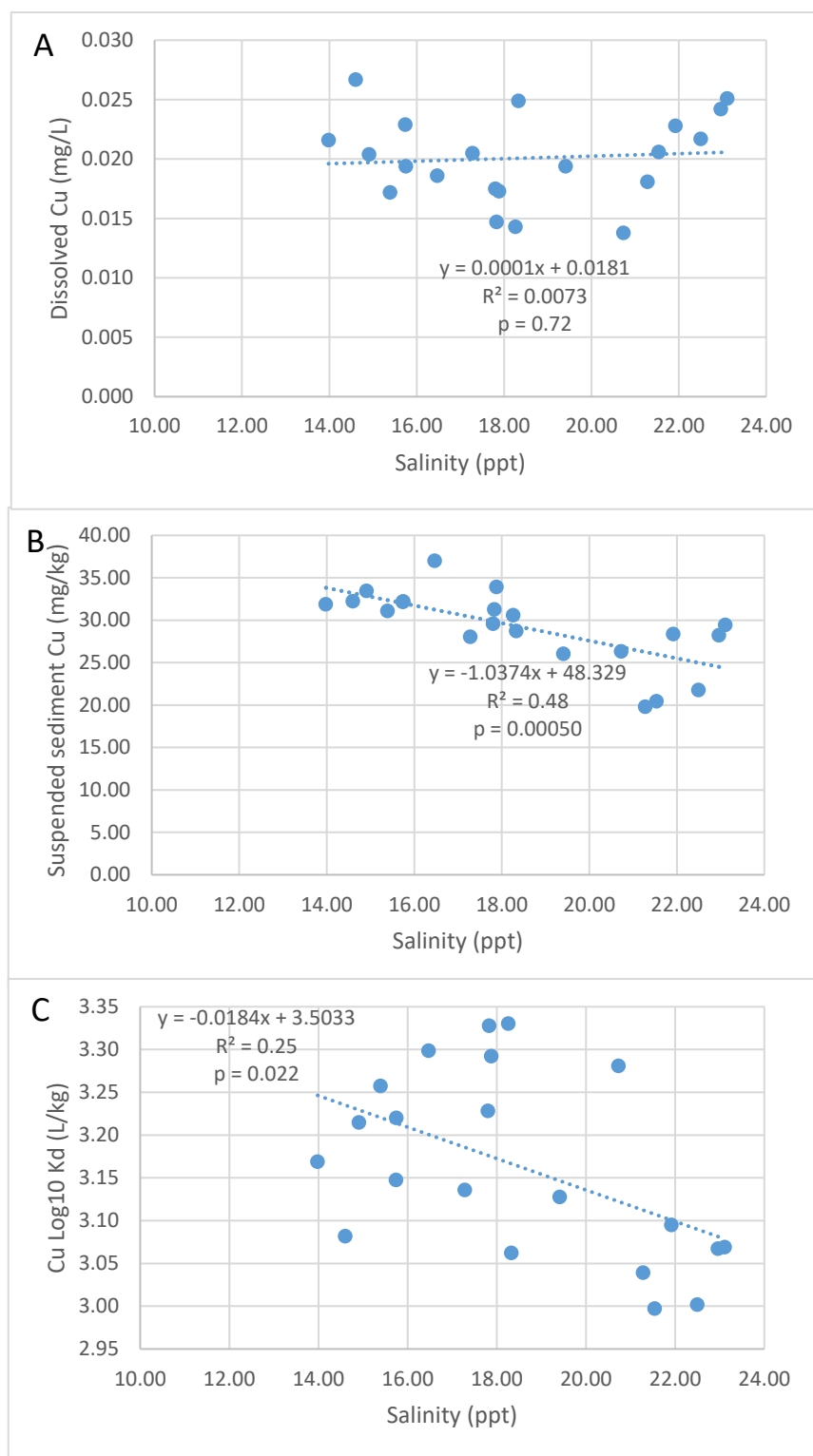


Figure B16: Dissolved (A), solid-phase suspended sediment (B), and K_d values of Cu (C) plotted against salinity. Linear regression lines are provided for each plot.

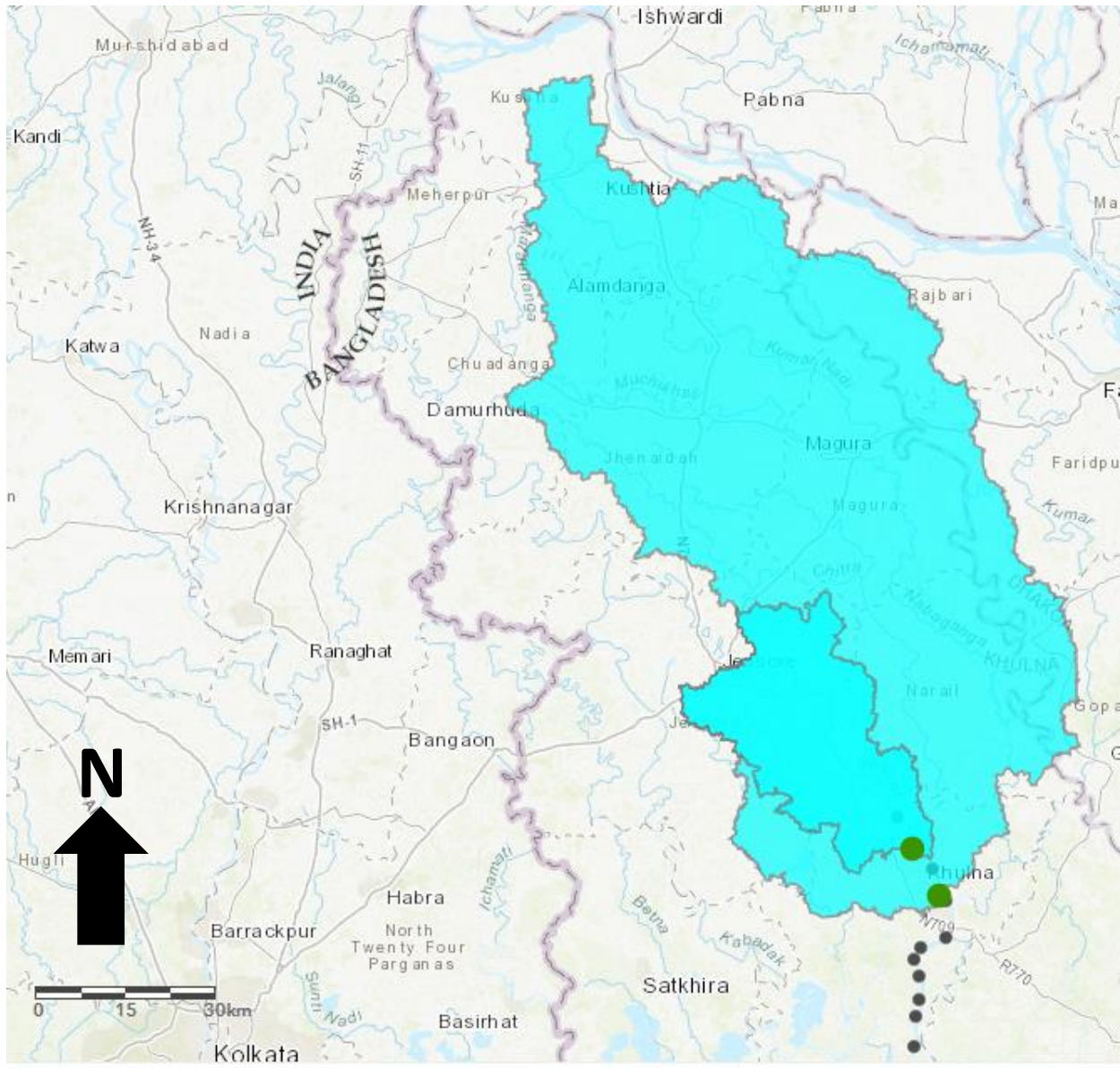


Figure B17: Watershed map for samples north of Khulna along the Bhairab River (smaller outlined watershed) and for samples south of Khulna along the Rupsha River (larger outlined watershed). Several sample sites are depicted as black dots, and the green dots represent the watershed drainage point.

Table B1: NIST standards 1646a (estuarine sediment) and 2702 (inorganics in marine sediment) run in duplicate on the ICP-OES under EPA Method 3051A to assess percent recovery of elements in sediments analogous to our suspended sediment samples. Percent recovery is only listed for elements that had either certified or reference mass fraction values listed within the standards.

Measured concentration (mg/kg)					% Recovery			
Element	1646a_1	1646a_2	2702_1	2702_2	1646a_1	1646a_2	2702_1	2702_2
Al	11080.0	11110.0	49690.0	50700.0	48.2	48.4	59.1	60.3
As	5.9	5.7	40.1	42.0	94.0	90.8	88.5	92.7
B	24.4	27.5	45.2	45.1				
Ba	37.0	35.9	162.2	167.8			40.8	42.2
Be	<0.851	<0.851	<0.851	<0.851				
Ca	3911.0	3966.0	2589.0	2632.0	75.4	76.4	75.5	76.7
Cd	1.0	1.1	4.5	4.6	704.1	728.4	554.0	566.7
Co	8.8	6.3	33.5	29.3			120.6	105.4
Cr	26.6	26.0	278.0	282.4	65.1	63.5	79.0	80.2
Cu	8.2	8.4	106.3	109.0	81.8	83.8	90.3	92.6
Fe	15810.0	16070.0	46480.0	47110.0	78.7	80.0		
K	3767.0	3735.0	12030.0	12360.0	43.6	43.2	58.6	60.2
Li	9.6	9.4	71.6	73.4				
Mg	3462.0	3469.0	8246.0	8529.0	89.2	89.4	83.3	86.2
Mn	164.8	165.8	1646.0	1682.0	70.3	70.7	93.7	95.7
Mo	1.2	1.0	7.1	6.7			65.6	62.3
Na	3994.0	4071.0	4140.0	4246.0	53.9	54.9	60.8	62.3
Ni	20.6	21.0	71.1	72.0			94.4	95.5
P	260.5	265.3	1397.0	1420.0	96.5	98.3	90.0	91.5
Pb	8.2	7.9	116.9	124.8	70.4	67.3	88.0	94.0
S	3203.0	3268.0	14380.0	14770.0	91.0	92.8		
Sb	<0.360	<0.360	7.1	6.7			126.4	120.3
Se	1.2	2.5	3.5	3.4	615.5	1296.9	69.8	68.7
Si	1862.0	1968.0	2368.0	2330.0	0.5	0.5		
Sr	24.0	23.8	64.2	67.1			53.6	56.1
Tl	<1.034	<1.034	<1.034	<1.034				
V	29.3	29.5	293.7	299.1	65.4	65.8	82.1	83.6
Zn	37.9	39.0	438.1	447.1	77.5	79.7	90.3	92.1

Table B2: Calculated Log10 Kd (bulk solid concentration/dissolved concentration) values (L/kg) used in this study (with MDLs used when suspended sediment values <MDL). The medians and standard deviations are also provided.

Sample ID	Al	Fe	V	Zn	Cr	Ni	Co	Cu	Ba	Mn	K	Ca	Sr	Na	Mg	Sb	As	Se	B	Cd	S
MD-TC-1	5.28	7.56	3.48	3.42	3.46	3.56	4.24	3.08	2.45	5.71	1.41	1.68	0.98	-0.15	1.36	3.36	2.06	1.21	0.63	4.28	0.31
MD-TC-2	5.23	6.75	3.45	3.78	3.40	3.47	4.22	3.26	2.43	5.65	1.38	1.46	0.91	-0.02	1.34	3.51	2.09	1.63	0.63	4.32	0.36
MD-TC-3	5.25	6.83	3.54	3.90	3.51	3.54	4.28	3.22	2.46	5.82	1.41	1.45	0.94	0.15	1.36	3.27	2.45	1.90	0.73	4.99	0.46
MD-TC-4	5.33	6.98	3.53	3.99	3.53	3.58	4.23	3.30	2.55	5.83	1.47	1.44	1.01	0.32	1.40	3.66	2.16	0.99	0.89	4.48	0.59
MD-TC-5	5.06	7.05	3.38	3.75	3.37	3.37	4.16	3.14	2.35	5.82	1.23	1.59	0.88	-0.04	1.24	3.39	2.27	1.00	0.46	4.19	0.34
MD-TC-6	5.23	6.91	3.46	3.81	3.47	3.40	4.18	3.23	2.45	5.78	1.30	1.69	0.92	-0.18	1.28	3.46	2.22	1.38	0.58	4.36	0.25
MD-TC-7	5.19	6.93	3.50	3.93	3.48	3.41	4.22	3.29	2.44	5.92	1.28	1.58	0.88	-0.12	1.28	3.59	2.23	0.95	0.57	4.49	0.28
MD-TC-8	5.20	6.88	3.52	3.84	3.49	3.43	4.23	3.33	2.47	5.95	1.30	1.58	0.90	-0.04	1.29	3.42	2.27	1.66	0.62	4.55	0.34
MD-TC-9	5.24	7.09	3.51	3.85	3.49	3.42	4.21	3.33	2.50	5.99	1.31	1.63	0.90	-0.25	1.28	3.63	2.19	1.05	0.59	4.31	0.27
MD-TC-10	5.00	7.01	3.40	3.72	3.37	3.29	4.13	3.13	2.40	5.88	1.13	1.52	0.78	-0.21	1.16	3.04	2.05	1.71	0.44	4.27	0.25
MD-TC-11	5.17	7.33	3.48	3.90	3.48	3.32	4.13	3.28	2.54	5.98	1.21	1.29	0.79	0.08	1.19	3.45	2.20	1.13	0.67	4.33	0.40
MD-TC-12	5.14	7.33	3.49	3.87	3.48	3.22	4.07	3.04	2.61	5.82	1.32	1.32	1.01	0.56	1.29	2.83	1.13	1.16	0.99	4.26	0.82
MD-TC-13	4.96	7.11	3.34	3.54	3.32	3.13	4.00	3.00	2.44	5.82	1.05	1.18	0.67	0.01	1.06	3.42	2.10	1.49	0.51	3.84	0.33
MD-TC-14	5.17	6.95	3.58	3.35	3.56	3.28	4.17	3.09	2.75	6.09	1.28	1.43	0.84	0.06	1.23	3.35	1.12	2.38	0.75	4.30	0.44
MD-TC-15	5.05	7.16	3.28	3.35	3.41	3.16	4.06	3.00	2.63	5.86	1.12	1.30	0.74	0.12	1.10	2.93	1.88	1.36	0.61	4.17	0.42
MD-TC-16	5.16	7.42	3.46	3.50	3.53	3.25	4.13	3.07	2.80	5.88	1.25	1.31	0.84	0.21	1.20	3.65	2.10	2.04	0.76	3.78	0.51
MD-TC-17	5.17	7.13	3.48	3.45	3.51	3.24	4.14	3.07	2.78	5.90	1.22	1.25	0.79	0.15	1.18	3.38	2.29	1.42	0.79	2.75	0.47
MD-TC-18	4.95	6.98	3.46	3.53	3.38	3.26	4.16	3.06	2.35	6.22	1.17	1.57	0.82	-0.22	1.19	3.37	2.19	2.84	0.40	4.28	0.28
MD-TC-19	5.26	6.83	3.68	3.67	3.60	3.51	4.35	3.15	2.50	6.27	1.47	1.61	0.98	-0.07	1.39	3.38	2.58	3.31	0.72	4.30	0.39
MD-TC-20	5.38	7.09	3.74	3.64	3.62	3.58	4.41	3.21	2.55	6.54	1.54	1.48	1.04	0.26	1.45	3.57	2.66	2.93	0.93	4.32	0.57
MD-TC-21	5.32	7.10	3.72	3.53	3.61	3.58	4.37	3.17	2.47	6.42	1.50	1.45	1.03	0.23	1.45	3.51	2.81	3.76	0.85	3.94	0.57
Median	5.19	7.05	3.48	3.72	3.48	3.40	4.18	3.15	2.47	5.88	1.30	1.46	0.90	0.01	1.28	3.42	2.19	1.49	0.63	4.30	0.39
Standard Deviation	0.12	0.21	0.11	0.20	0.08	0.14	0.10	0.11	0.13	0.23	0.13	0.15	0.10	0.21	0.11	0.22	0.40	0.82	0.16	0.42	0.14

Table B3: Trace element concentrations in surface water samples in recent studies in Southwest Bangladesh.

As ¹	Cd	Cu	Cr	Fe	Mn	Ni	Pb	Zn	Months of sampling	Location	Study
57.0	0.1	20.2	13.7	2.6	0.7	16.7	<MDL	16.5	May	Bhairab-Rupsha-Bhadra-Shibsa Rivers	This study
8.0				98.0					June-Aug	Ponds/Lakes in Rupsha Upazila	Ahmed et al. (2020)
3.5	6.5		45.2	976.6	288.5	18.7	18.4	68.4	March-May	Rupsha River Basin	Islam et al. (2020)
12.3	9.8		40.0	2062.0	65.4	21.4	26.6	33.8	March-May	Pasur River Basin	Islam et al. (2020)
5.5	1.0	5.4	7.2			3.9	7.1		Aug-Sept	Rupsha River	Proshad et al. (2020)
6.1	1.4	6.0	8.9			5.5	7.3		Jan-Feb	Rupsha River	Proshad et al. (2020)

¹All concentrations are mean values, in µg/L.

References

- Ahmed, A., Ghosh, P. K., Hasan, M., & Rahman, A. (2020). Surface and groundwater quality assessment and identification of hydrochemical characteristics of a south-western coastal area of Bangladesh. *Environmental monitoring and assessment*, 192(4), 1-15. <https://doi.org/10.1007/s10661-020-8227-0>
- Dietrich, M., & Ayers, J. C. (2021). Influences on tidal channel and aquaculture shrimp pond water chemical composition in Southwest Bangladesh. *Geochemical Transactions*, 22(1), 1-22. <https://doi.org/10.1186/s12932-021-00074-2>
- Gaillardet, J., Viers, J., Dupré, B. (2014). Trace Elements in River Waters in: Surface and Ground Water, Weathering and Soils, *Treatise on Geochemistry*. <https://doi.org/10.1016/B978-0-08-095975-7.00507-6>
- Hale, R., Bain, R., Goodbred Jr., S., & Best, J. (2019). Observations and scaling of tidal mass transport across the lower Ganges–Brahmaputra delta plain: Implications for delta management and sustainability. *Earth Surface Dynamics*, 7(1), 231–245. <https://doi.org/10.5194/esurf-7-231-2019>
- Islam, A. R. M. T., Islam, H. T., Mia, M. U., Khan, R., Habib, M. A., Bodrud-Doza, M., ... & Chu, R. (2020). Co-distribution, possible origins, status and potential health risk of trace elements in surface water sources from six major river basins, Bangladesh. *Chemosphere*, 249, 126180. <https://doi.org/10.1016/j.chemosphere.2020.126180>
- Mason, R. P. (2013). Trace metals in aquatic systems. John Wiley & Sons.
- Proshad, R., Islam, S., Tusher, T. R., Zhang, D., Khadka, S., Gao, J., & Kundu, S. (2020). Appraisal of heavy metal toxicity in surface water with human health risk by a novel approach: a study on an urban river in vicinity to industrial areas of Bangladesh. *Toxin Reviews*, 1-17. <https://doi.org/10.1080/15569543.2020.1780615>